Mustansiriyah Journal of Pure and Applied Sciences

www.MJPAS.com

Natural Radioactivity Mapping in Soil Samples of Salah al-Din and Anbar Regions – Iraq Using GIS Technique

Emad Hameed Ahmed[1], Mahmood Salim Karim[2], Fouad Kadam Mashi[3]

1. Department of Physics, College of Science, Mustansiriyah University : Correspondent author email: emadhameed321@uomustansiriyah.edu.iq
2. Department of Physics, College of Education, Mustansiriyah University
3. Department of Physics, College of Science, Baghdad University

A B S T R A C T

This study aims to identify and depict natural radiation levels (uranium-238, thorium-232, and potassium-40) in soil samples obtained from the Iraqi governorates of Salah al-Din and Anbar. The (HPGe) detector was used in the detection system of the investigation, and maps were created using a geographic information system (GIS). Some radiological characteristics were computed based on particular activity measurements for 238U, 232Th, and 40 K. Specific activity averages are 20.422 Bq/kg for 238U, 23.008.6 Bq/kg for 232Th, and 178.726 Bq/kg for 40K. Furthermore, the radium equivalent (Raeq), absorbed dose rate (Dg), external hazard index (Hex), internal hazard index (Hin), representative gamma hazard index (I_γ), and total annual effective dose equivalent (AEDE) are estimated to be 67.085 Bq/kg, 30.784nGy/h, 0.181, 0.236, 0.243 and 0.083 mSv/y respectively. The specific activity of Uranium-238, Thourium-232, and Poasium-40 identified in all soil samples was under the UNSCEAR safety level. For the study region, GIS mapping for natural radioactivity and several radiological criteria were generated effectively. Finally, the Natural radioactivity and radiation properties of soil samples from Salah al-Din and Anbar were harmless.

Keywords: *Concentrations of radioactive elements, nuclear facility, Geographic Information System (GIS) and Interpolation Technique (IDW).*

Corresponding author : Emad Hameed Ahmed
E-mail address: emadhameed321@uomustansiriyah.edu.iq

1. Introduction

Natural radioactivity is typical and can be found in various geological formations and rocks. The importance of this study is centered on the radiation effect, which is of significant interest and significance in the field of health physics; thus, Determining the degree of change in the radioactive setting over time owing to radioactive impact propagation requires measuring natural radioactivity in sediments. [1]. The soil is a source of sustenance for humans and one of the significant contributors to radiation exposure. As a result, it is critical to investigate the distribution of natural radioactivity in soil and sediments [2]. Natural radioactive materials (NORM) research how the environment is impacted by biochemical and geochemical indicators linked to geological phenomena like earthquakes and volcanic eruptions. The described natural radioactivity is mainly caused by the presence of the 238U, 232Th series, and 40K during the weathering and deposition of sediments [3]. The principal external cause of irradiation of the human body is gamma radiation generated by these naturally occurring radionuclides.

In contrast, radon gas inhalation and its quick-decaying byproducts cause interior exposure. 238U, 232Th, and 40K have average specific activities of 30, 33, and 400 Bq/kg, respectively [4]. Geological circumstances primarily determine the natural environmental radioactivity caused by gamma-radiation, and it disperses at varying quantities of radionuclides in the world's soils and sediments [5]. Many contamination studies worldwide have been interested in measuring the particular activity of natural substances.

2. The study area

A-Anbar city

Anbar Governorate is a governorate in Iraq located in western Iraq. It is Iraq's largest province, covering the equivalent of one-third (1/3) of the country's land area. It contains the west plateau, which reaches more than 900 meters above sea level in the shortest west of Anbar, as shown in Figure 1. The Euphrates River rises 375 meters above sea level (200 meters above ground). Many valleys may be found along Wadi and Hauran and near Al-Rutba. It is bounded to the north by the governorates of Salah al-Din and Nineveh and to the northwest by the Syrian Arab Republic. Jordan lies to the west. The province of Baghdad from the east. To the south is the Kingdom of Saudi Arabia, and the regions of Karbala and Najaf to the southeast. West of Iraq is where the province of Al-Anbar is situated, and its astrological location is limited between latitudes (31 and 35) in the north and longitudes (39 and 44) in the east [6].

B-Salah-al dine city

Salah al-Din Governorate is an Iraqi governorate located north of Baghdad in central Iraq. Tikrit is the city at its heart. Samarra is the country's largest city. The governorate is astronomically positioned at 43.35 degrees east of the Greenwich meridian and 34.27 degrees north of the equator, with a land area of 24,363 km2. Salah-el-Din governorate is located

northwest of Baghdad governorate and southeast of Ninavah governorate. Kirkuk and Diyala governorates are to the east, while the Anbar governorate is to the west [7]. Tikrit, Shirqat, Baiji, Samarraa, Balad, and Dour are the six cities in Salah-el-din governorate. Each such city is affiliated with several towns. The governorate is well-known for its agriculture of various crops, as shown in Figure 2.

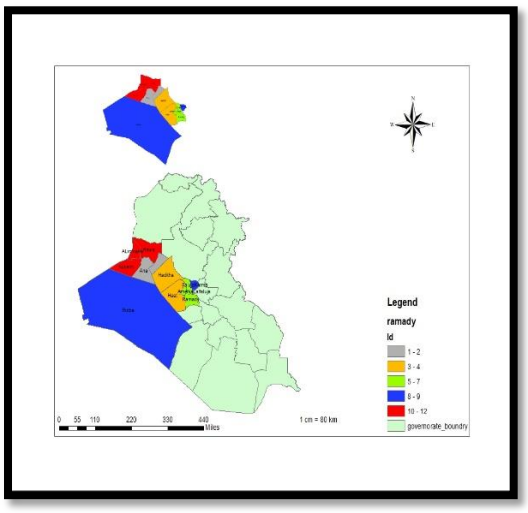

Figure.1 Anbar city

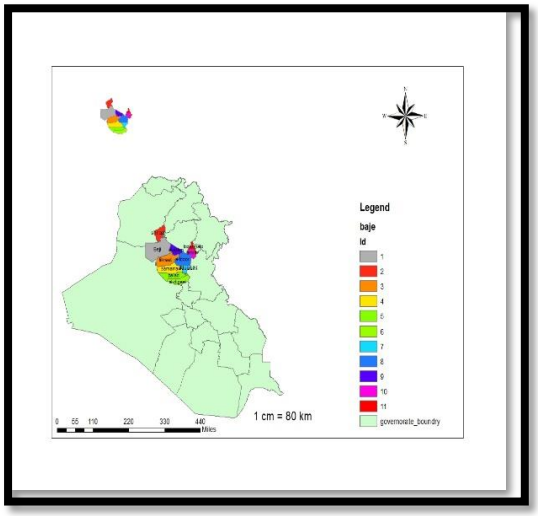

Figure.2 Salah-al Dine City

3-Materials and method

This study used geographic information systems, and the two governorates under investigation were merged into one form, as in Figure 3. Some districts were excluded, representing large desert areas that are not useful in this study. The Global Positioning System (GPS) device was utilized to achieve exceptional accuracy in identifying each Sample on the ground and projecting it onto the Geographic Information System (GIS) software package to record and manage these results, as shown in Table 1.

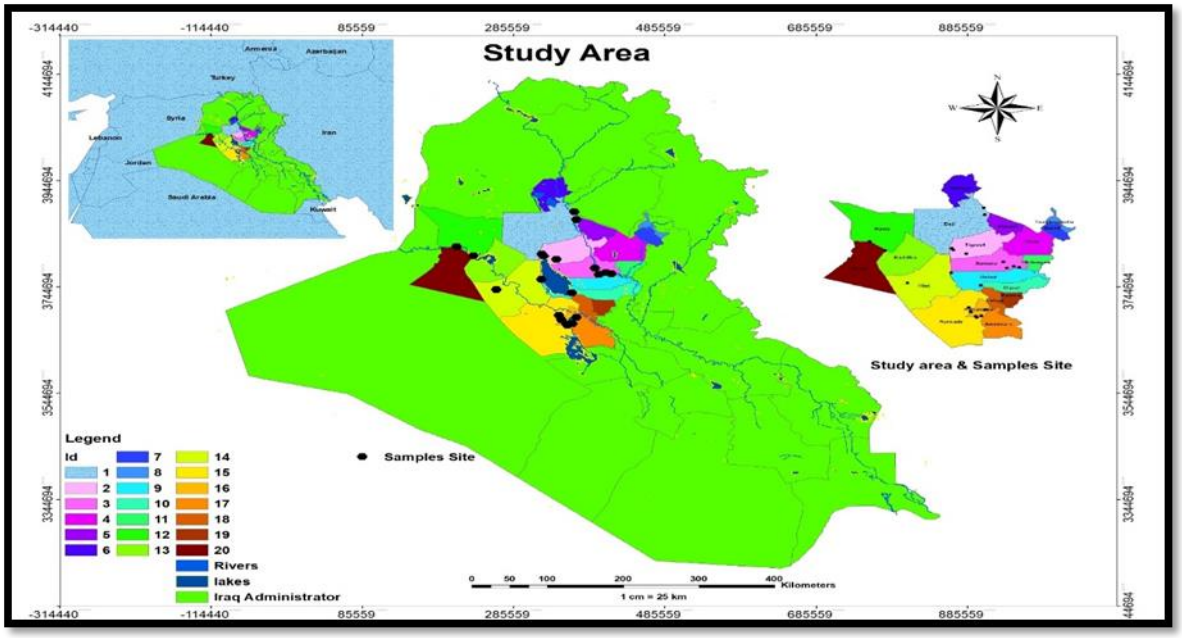

Figure. 3(study area)

Table 1. Names and locations of the current study's soil samples, together with their coordinates

No	City name	x-coordinate	y-coordinate
1	Habaniea	362926.152	3675321.658
2	Habanyea	356696.525	3672309.370
3	Habanyea	354916.365	3674461.565
4	Ramady	348775.259	3682283.191
5	Habanyea	345425.714	3691472.808
6	Rawa	210366.235	3819843.606
7	Faluja	362203.877	3733802.103
8	Alfurst(Hiet city)	321693.089	3758615.659
9	Habanyea	368610.506	3687250.782
10	Tikrit	342083.242	3796375.817
11	Hadtha	232355.609	3802719.565
12	Kubesa(Hiet city)	262190.956	3739207.617

13	Tikrit	324825.915	3803262.311
14	Tikrit	322936.786	3806453.193
15	Beji	365875.439	3885826.014
16	Beji	368157.475	3871240.829
17	Samara	392896.066	3779827.104
18	Samara	393187.744	3768185.415
19	Almuhtasam (Samara)	414591.943	3769243.750
20	Almuhtasam (Samara)	407543.469	3771005.420

4.1.- gathering and getting ready of samples

Twenty soil samples were obtained from selected regions in Anbar and Salah al-Din governorates. All models were taken from the soil at a depth of 10 cm. Each soil sample was stored in a plastic pouch and labeled with the location where it was gathered. All models were dried by the sun's heat to remove extra wetness. To achieve homogeneity, an electric mill was used to smash the models. The samples were sieved and stored in a plastic bag to keep them dry. They were baked for roughly an hour in an electric oven to produce a consistent weight. Nuclear Physics Laboratory, Physics Department, Faculty of Education, University of Mustansiriyah, has concluded work on experimental measurements. To achieve geometric uniformity around the detector, Marinelli beakers (1 L) of consistent volume were used to load the samples. After that, the net weights were computed. Using a digital scale to weigh and measure to establish equilibrium, the plastic Marinelli beakers were employed. Taped closed and stored for approximately four weeks before attempting to attain secular stability [8].

4.2. Gamma-ray Spectroscopy Detection System

In this work, the detection method for gamma rays is based on the interaction of gamma-ray photons with the detector material. Within the detector volume, any of the (primary) forms of gamma-ray interactions can occur, though the photoelectric effect and Compton scattering are the most recognized types that play essential roles in photon detection. [9]. The primary gamma-ray photons and/or secondary scattered photons interact with the detector atoms and create fast electrons with energy proportionate to the source photon inside the detector volume for these interactions. These speedy electrons can combine to generate secondary electrons as they travel through the detector region. Electrical pulses can be caused by capturing secondary and tertiary electrons. To alter the charges, a pre-amplifier might be utilized. A pre-amplifier converts the leads to a voltage whose magnitude is proportionate to the original gamma-ray energy. A functional gamma spectroscopy detector must perform two

independent roles. First, the detector must function as a radiation converter medium with a reasonable probability of interaction to generate fast electrons, which must be able to travel easily through the detector; second, the detector's background noise must be low enough to collect only those electrons that represent the energy of the detected gamma-ray photons. These can be attained if the detector can withstand a high electric field while operating at a low temperature [10].

5. Theoretical calculations

Specific Activity. A sample's activity is measured in terms of Bq/g or Ci/g of activity per unit mass. The following equation is used to estimate each Sample's unique activity: [11]:

$$A_i(E_\gamma) = \frac{N}{t_c \times I_\gamma(E_\gamma) \times \varepsilon(E_\gamma) \times M} \quad (1)$$

Where:

$A_i(E_\gamma)$: radionuclide-specific activity measured in (Bq/kg) or (Bq/l). N: the net peak area beneath the peak, which equals (Total counts - Background counts). t_c Is the counting lifetime equal to (3600 s). $I_\gamma(E_\gamma)$: the abundance of energy E_γ. $\varepsilon(E_\gamma)$: is the detection efficiency at energy E_γ . M: the mass of the soil and oil sample (kg) or (liter).

Radium Equivalent Activity (Ra_{eq}). Ra_{eq} is used to obtain the sum of 238U, 232Th, and 40K activities, and The following equation gives the radium equivalent training in Bq/kg units.: [12]:

$$Ra_{eq(Bq/kg)} = A_u + 1.43A_{Th} + 0.077A_k \quad (2)$$

where A_U, A_{Th}, and A_K. are the radionuclide's particular actions 238U, 232Th, and 40K, respectively

Annual Effective Dose Equivalent

With an outdoor occupancy of 20%, the estimated yearly effective dose equivalent received by a person was determined using a conversion factor of (0.7 Sv/Gy) to convert the absorbed rate to human effective dose equivalent and an interior occupancy of (80%), as well as the accompanying relationships. [13]:

$$(AED)in(msv/y) = D_\gamma(nGy/h) \times 10^{-6} \times 8760(h/y) \times 0.80 \times (0.7\, sy/Gy) \quad (3)$$

$$(AED)out(msv/y) = D_y(nGy/h) \times 10^{-6} \times 8760(h/y) \times 0.20 \times (0.7\, sy/Gy) \quad (4)$$

Sometimes, the above two abbreviations might be written as $(AEDE)_{in}$ and $(AEDE)_{out}$.

External Annual Effective Dose (EAD)

The external annual effective dose was obtained by using the following relation [14]:

$$EAD = (0.92A_u + 1.1A_{Th} + 0.08A_k) \times (10^{-9}\, Gy/h) \times (0.7\, sv/Gy) \times (24 \times 365\, h/y) \times 0.8 \quad (5)$$

Activity Concentration Index (I_γ)

The activity index (I_γ) for soil samples was calculated by using the following relation [14]:

$$I_\gamma = \frac{A_u}{150} + \frac{A_{Th}}{100} + \frac{A_k}{1500} \quad (6)$$

External (H_{ex}) and Internal (H_{in}) Hazard Indices

The internal hazard index (H_{in}) is given by the following relation [15]:

$$H_{in} = \frac{A_u}{185} + \frac{A_{Th}}{259} + \frac{A_k}{4810} \quad (7)$$

The external hazard index (H_{ex}) is given by the following relation [15]:

$$\boldsymbol{H_{ex} = \frac{A_u}{370} + \frac{A_{Th}}{259} + \frac{A_k}{4810}} \quad (8)$$

These indices readings must be less than one for the radiation threat to be considered minimal.

6. Result and discussion

The outcomes of specific activity of natural radionuclides (238U, 232Th, and 40K) in soil for study area districts were shown in Table 2. The findings of the radiological parameters (Ra_{eq}, H_{ex}, H_{in}, and I_γ) and (Exposure, Dr, AGED, and AEDE outside,) respectively, are shown in Tables 3 and 4. In the examined region, uranium-238 specific activity ranged from 9± 1 Bq/kg to 26±1 Bq/kg, with an average value of 20±1, from 14±1 Bq/kg to 30.1±1 Bq/kg with an average 23±1 Bq/kg for thorium-232, from 273.5±1 Bq/kg to 100±1 Bq/kg having a mean value of 178±1 Bq/kg for potassium-40, The most significant possible value of the specific activity of 238U, 232Th, and 40K was seen in the Sample no 15 (Bije), while 232Th was in Sample no 17 (samara). The smallest specific activity value of 238U, 232Th, and 40K was found in samples 2,2 and 2, respectively. However, the average concentration of thorium-232 in the study area is nearly higher than that of uranium-238. The gap between 238U and 232 Th concentrations represents the minimal monazite minerals in the samples. Because 232Th activities are typically more extensive than 238 U occurrences in the crust, where soil originates, the values are almost less than unity. These differences may exist because the decay series for uranium and thorium derive from distinct origins and coexist in nature, while the decay series for potassium is from a separate source. [16, 17]. The availability of agricultural land and locations with phosphate fertilizers, where peer-potassium (40 K) is becoming increasingly important, is the reason for the highest distribution of potassium-40, even though the potassium nuclide concentration may be growing in some areas. According to recommendations by UNSCEAR 2008, the average values of the specific activity of 238U,

232Th, and 40 K were 33 Bq/kg, 45 Bq/kg, and 420 Bq/kg, respectively [18]. As a result, UNSCEAR 2008 encompassed the precise 238U and 232Th activity indicated in Table 2 at all geographic locations. Used geographic information system (GIS) technology... to create a distribution map of the specific activities for radioisotopes 238U, 232Th, and 40K in all soil samples included in the current investigation, each measured in Bq/kg.

Table 2. The particular soil activity for study region districts' natural radioactivity

No.	U-238 (Bq/Kg)	Th-232 (Bq/Kg)	K-40 (Bq/Kg)
1	12.620	16.660	103.570
2	9.070	14.110	100.840
3	11.740	23.810	111.530
4	14.470	23.430	123.190
5	20.390	16.550	153.360
6	21.020	21.810	135.080
7	20.870	26.520	217.610
8	19.440	25.520	220.550
9	23.050	24.670	176.920
10	22.410	24.120	202.330
11	23.870	22.830	123.530
12	19.440	20.380	133.850
13	25.450	22.530	231.540
14	22.330	23.640	243.490
15	26.070	29.150	273.560
16	22.430	23.820	185.870
17	24.550	30.380	207.650
18	24.440	24.540	242.650
19	25.450	23.370	196.960
20	19.320	22.320	190.430

avr	**20.422**	**23.008**	**178.726**
min	**9.070**	**14.110**	**100.840**
max	**26.070**	**30.380**	**273.560**
#VALUE!	**3.688**	**2.687**	**44.666**

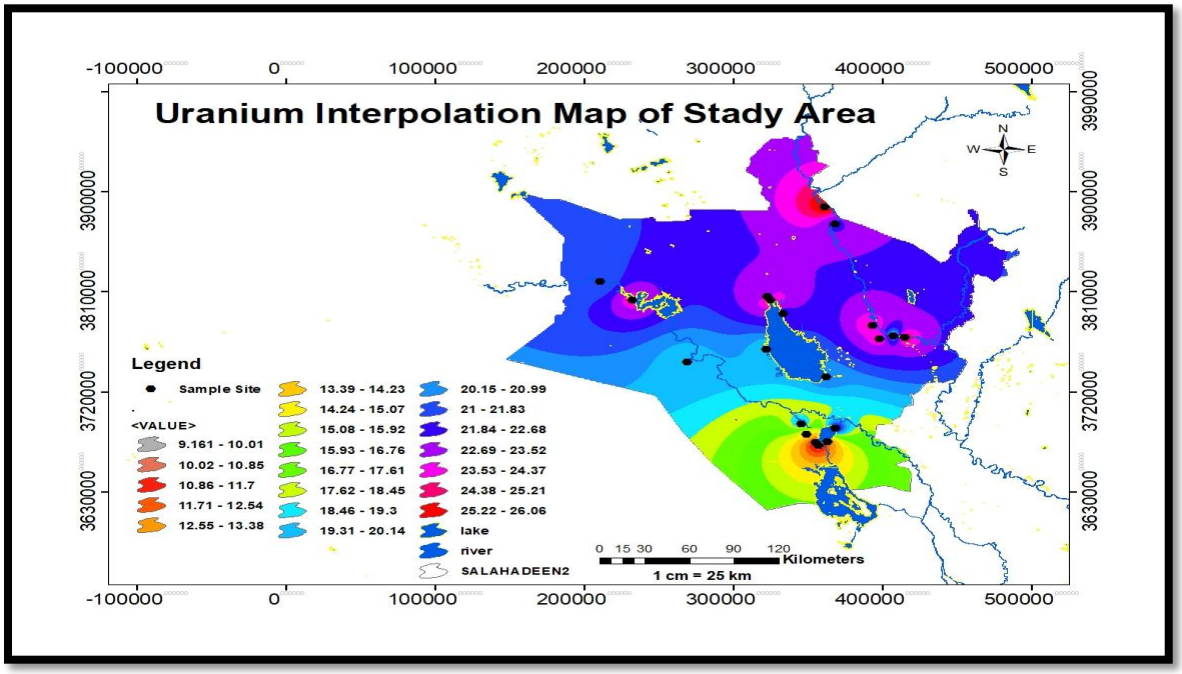

Figure 4. The distribution of 238 U in the soil of the research area.

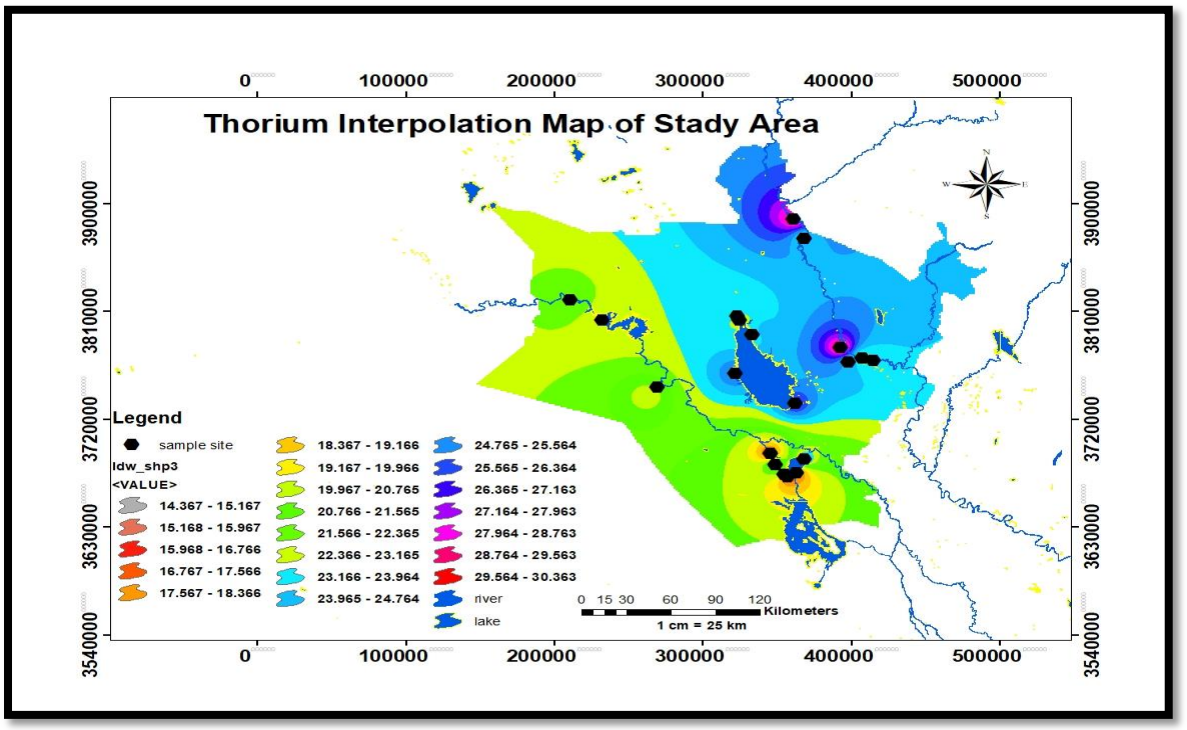

Figure5. The distribution of 232 Th in the soil of the research area.

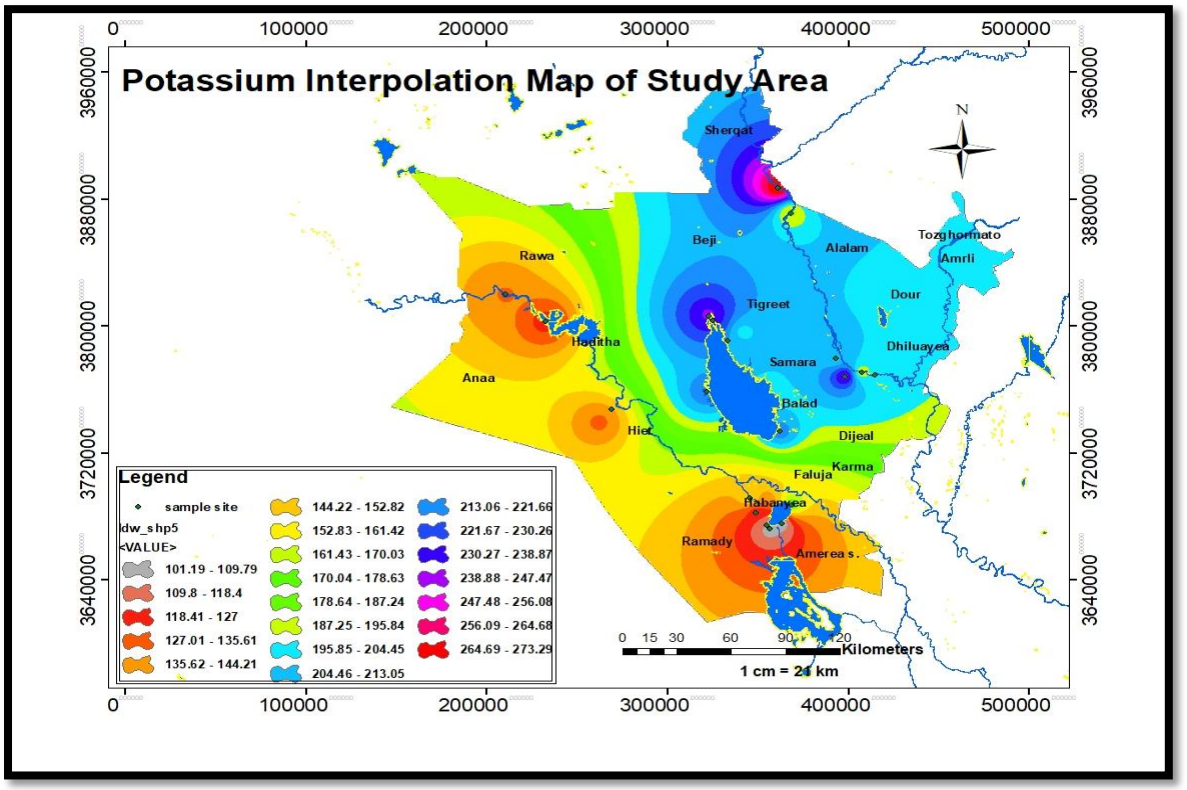

Figure 6. The distribution of 40 K in the soil of the research area.

The Ra_{eq} results varied from 37.012 Bq/kg to 88.819 Bq/kg, with a mean value of 67.085 Bq/kg. The lowest and highest values of H_{ex}, H_{in}, and I are likewise reported in Table 3. Hex and Hin values varied from 0.100 to 0.240, based on an average of 0.181, and from 0.124 to 0.310, with an average of 0.236. Other parameters, such as I, have results ranging from 0.134 to 0.324, with an average of 0.243. Radiological variables (Ra_{eq}, H_{ex}, H_{in}, and I_{γ}) in Table 3 were less than for all soil samples under investigation, 370 Bq/kg for Ra_{eq} [19] and less than unity for H_{ex}, H_{in}, and I [20].

Table 3. The radiological parameters for natural radioactivity in soil (Ra_{eq}, E_{in}, E_{out}, I_{γ}, H_{ex}, and H_{in}) for study area districts

No.	Ra_{eq} (Bq/Kg)	E_{in} (mSv/y)	E_{out} (mSv/y)	I_{γ}	H_{in}	H_{ex}
1	44.41869	0.0991517	0.0247879	0.15989	0.1540728	0.1199647
2	37.01198	0.082992	0.020748	0.1343967	0.1244704	0.0999569
3	54.37611	0.119971	0.0299927	0.19536	0.1785771	0.1468473
4	57.46053	0.1274175	0.0318544	0.2064467	0.1942908	0.1551827
5	55.86522	0.1266209	0.0316552	0.2018367	0.2059994	0.1508913
6	62.60946	0.1398945	0.0349736	0.2241433	0.2259133	0.1691025
7	75.54957	0.1703929	0.0425982	0.2747033	0.2604458	0.2040404
8	72.91595	0.1647904	0.0411976	0.2659167	0.2494663	0.1969257
9	71.95094	0.1615284	0.0403821	0.2591567	0.2566273	0.19433
10	72.48101	0.1636462	0.0409116	0.2627433	0.256327	0.1957594
11	66.02871	0.1470133	0.0367533	0.2348933	0.2428557	0.1783421
12	58.88985	0.131825	0.0329562	0.2113167	0.2115958	0.1590552
13	75.49648	0.1718002	0.04295	0.2746633	0.2726932	0.2039094
14	74.88393	0.1704625	0.0426156	0.2737967	0.2625985	0.2022471
15	88.81862	0.201416	0.050354	0.3238367	0.3103404	0.2398809
16	70.80459	0.1594355	0.0398589	0.2558233	0.2518548	0.1912331
17	83.98245	0.1881328	0.0470332	0.30295	0.2931705	0.2268191
18	78.21625	0.1777394	0.0444349	0.28505	0.2773041	0.2112501
19	74.03502	0.1672153	0.0418038	0.2673367	0.2687473	0.1999635

20	65.90071	0.1488754	0.0372188	0.2394767	0.2302005	0.1779843
avr	67.084804	0.151016	0.037754	0.2426868	0.2363775	0.1811843
min	37.01198	0.082992	0.020748	0.1343967	0.1244704	0.0999569
max	88.81862	0.201416	0.050354	0.3238367	0.3103404	0.2398809

7. Conclusions

The specific activity values of 238U, 232Th, and 40K in the field project research area are within the identified global average values by specialist scientific bodies and organizations such as UNSCEAR, 2008. radiological risk outcomes (Ra_{eq}, H_{ex}, H_{in}, I_{γ}, and AEDE) are within worldwide limits (UNSCEAR, 2000; UNSCEAR, 2008; OECD and ICRP reports). As a result, it is possible to deduce that no population living in the research zone is at risk from harmful radiation impacts. The Global Positioning System (GPS) device was used to obtain extreme accuracy in locating each Sample on the ground and projecting it onto the Geographic Information System (GIS) software package to record and manage these readings and analyze the geographical locations so that they could be dealt with to apply the interpolation technique (IDW) to extract predictive maps on the concentrations of these radioactive elements.

Reference

1. M. Hasan et al. Natural Radioactivity and Assessment of Associated Radiation Hazards in Soil and Water Samples Collected from in and around the Barapukuria 2 × 125 MW Coal Fired Thermal Power Plant, Dinajpur, Bangladesh. Journal of Nuclear and Particle Physics 4(1) (2014) 17.
2. Rajesh, S., Avinash, P., Kerur, B. R., & Anilkumar, S. (2015, August). Assessment of natural radioactivity concentrations and gamma dose levels around Shorapur, Karnataka. In *AIP Conference Proceedings* (Vol. 1675, No. 1). AIP Publishing.
3. K. Thabayneh, M. Jazzar. Natural radioactivity levels and estimation of radiation exposure in environmental soil samples from Tulkarem Province-Palestine. Open Journal of Soil Science 2(01) (2012) 7.
4. A.A. Abojassim, H.H. Al-Gazaly, S.H. Kadhim. Estimated the radiation hazard indices and ingestion effective dose in wheat flour samples of Iraq markets. Intern. Journal of Food Contamination 1(1) (2014) 6.
5. S.C. Bushong. Radiologic Science for Technologists: Physics, Biology, and Protection (Elsevier Health Sciences, 2013).
6. Al-Mohamdi,Y.H , Maklf,A.L." The foundations of natural development in Al-Anbar governorate " Journal of College of Anbar Education, Anbar University, 1, pp.104-118, (2012).
7. Jassim, S.Z. and Goff, J.C. 2006. Geology of Iraq, Dolin, Prague and Moravian Museum, Berno. 341pp.

8. Abojassim, A. A., Hamad Al-Gazaly, H., Sabah Obide, E., & Madlool Al-Jawdah, A. (2020). Radioactivity in samples of cleaning materials. International Journal of Environmental Analytical Chemistry, 100(1), 99-108.
9. Knoll Glenn F.," Radiation Detection and Measurements," 3rd ed., NewYork: John Wiley & Sons, Inc. ISBN: 0-471-07338-5, (2000).
10. Krane, Kenneth S., " Introductory nuclear physics, "Kenneth S. Krane, Chichester: Wiley. New York, (1988).
11. A.A. Mirza, H.H. Al-Gazaly, A.A. Abojassim. Radioactivity levels and radiological risk assessment in Ur residential complex soil samples at Nassariya Governorate, Iraq. Pollution Research 36(4) (2017) 742
12. J. Beretka, P.J. Matthew. Natural radioactivity of Australian building materials, industrial wastes, and byproducts. Health Physics 48(1) (1985) 87.
13. Sam, A.K. and Abbas, N., "Assessment of radioactivity and associated hazards in local and imported cement types used in Sudan," J. of Radiation Protection Dosimetry, 88, pp. 225-260, (2010).
14. Ashraf, E.M.K; H.A. Layia; A.A. Amany and A.M. Al-Omran." NORM in clay deposits, "Proceedings of Third European IRPA Congress 2010 June 14-18, Helsinki, Finland, pp 1-9, (2010).
15. Silk, T.J.; Kendell, G.M. and Phipps, A.W., "Revised estimates of dose from ores and mineral sands, "J. of Radiol. Prot. 15, pp 217–222, (1995).
16. Abojassim, A. A., & Rasheed, L. H. (2021). Natural radioactivity of soil in the Baghdad governorate. Environmental Earth Sciences, 80(1), 1-13.
17. Tanasković, I., Golobocanin, D., & Miljević, N. (2012). Multivariate statistical analysis of hydrochemical and radiological data of Serbian spa waters. Journal of geochemical exploration, 112, 226-234.
18. UNSCEAR. (2008). Sources and effects of ionizing radiation: Report to the general assembly (United Nations, New York), with scientific annexes,2,1-219.
19. Nuclear Energy Agency. (1979). Exposure to radiation from the natural radioactivity in building materials: report. OECD.
20. Kaiser, S. (1999). Radiological protection principles concerning the natural radioactivity of building materials. Radiation Protection, 112.